

See discussions, stats, and author profiles for this publication at: <https://www.researchgate.net/publication/231396273>

Analysis of the Temperature Dependence of the ^1H Contact Shifts in Low-Spin Fe(III) Model Hemes and Heme Proteins: Explanation of "Curie" and "Anti-Curie" Behavior within the Same...

ARTICLE in THE JOURNAL OF PHYSICAL CHEMISTRY · DECEMBER 1995

Impact Factor: 2.78 · DOI: 10.1021/j100050a020

CITATIONS

78

READS

43

2 AUTHORS, INCLUDING:



F(rances) Ann Walker

The University of Arizona

242 PUBLICATIONS 8,684 CITATIONS

SEE PROFILE

Analysis of the Temperature Dependence of the ^1H Contact Shifts in Low-Spin Fe(III) Model Hemes and Heme Proteins: Explanation of “Curie” and “Anti-Curie” Behavior within the Same Molecule

Nikolai V. Shokhirev* and F. Ann Walker*

Department of Chemistry, University of Arizona, Tucson, Arizona 85721

Received: August 25, 1995[⊗]

The reasons that the temperature dependence of the NMR isotropic shifts of model ferrihemes and ferriheme proteins deviate from Curie behavior have been analyzed by considering the energies of the valence orbitals of the metal and the porphyrinate. For low-spin Fe(III), overlap of the e-symmetry π orbitals of a symmetrical porphyrin ring and the d_π orbitals of the metal produces two low-energy molecular orbitals that are mainly porphyrin in character and are filled and two high-energy (valence) molecular orbitals that are mainly metal in character and contain three electrons. The odd electron in the valence set thus gives rise to the spin delocalization that results in the observed contact shift pattern of these systems. Unsymmetrical substitution and/or presence of a planar axial ligand that is prevented from rotation removes the degeneracy of these e(π) orbitals, producing a system in which the energy separation between the two formerly degenerate π orbitals, ΔE_π , is of the order of only tens of cm^{-1} for the former or quite large (several times $k_B T$) for the latter. In either case, both orbitals are utilized for spin delocalization to a significant extent as the temperature is varied, according to their varying Boltzmann populations. Such a two-level system obeys a modified Curie law that takes into account the thermal population of the two levels as a function of temperature. In fact, the temperature dependence of some of the contact shifts of model hemes or heme proteins may show anti-Curie behavior if ΔE_π is large compared to $k_B T$ at ambient temperatures. Such anti-Curie behavior has been observed for two of the heme methyl resonances of several cytochromes *c* and *b₅* and cyanometmyoglobins or -hemoglobins, where the axial methionine π -symmetry lone pair or histidine imidazole plane orientation, respectively, is believed to be the important factor in determining ΔE_π . Assuming reasonable energy separations of the two valence e(π) orbitals, from very small to quite large ($\sim 1000 \text{ cm}^{-1}$), the expected temperature dependence of the contact shifts has been calculated for an assumed set of valence MO coefficients. These results have then been compared to the experimental isotropic shifts of several model heme systems having unsymmetrical substitution patterns and/or one fixed axial ligand and to several heme proteins. Using a computer program developed to fit the observed isotropic shifts to the two-level equation, ΔE_π was estimated from the temperature dependence of the isotropic shifts of the protons of the β -pyrrole substituents of the above-mentioned systems. In the case of the proteins investigated, *Aplysia* cyanometmyoglobin and cytochrome *b₅*, the values of ΔE_π obtained from analysis of proton isotropic shifts are similar to those calculated from EPR *g* values measured at low temperatures, while for model hemins, the values of ΔE_π obtained are smaller than those predicted and vary in accord with the expectations as to the rigidity, or lack thereof, of the orientation of at least one planar axial ligand, indicating that thermal averaging of the two levels due to rapid rotation (or libration) of the axial ligand is fast on the NMR time scale. This same two-level approach could be applied to any system in which there is a thermal equilibrium between two states separated by an energy within several factors of $k_B T$.

Introduction

For some time we have been interested in two factors that may affect the size and pattern of the contact shifts of low-spin iron(III) model hemes and heme proteins: (1) heme substituents^{1–7} and (2) axial ligand plane orientation.^{7–12} Both of these factors have been shown to be important in determining the proton NMR shifts of heme proteins,^{13–27} as well as other spectroscopic and redox properties. In particular, it has been suggested that axial ligand plane orientation not only determines the pattern and spread of pyrrole-substituent resonances but may also modulate reduction potentials,^{8,30} especially within the cytochromes that contain two axial histidine ligands that may, in the extremes, be aligned in parallel or perpendicular planes. The reason for this is that the 3e(π) orbitals of the porphyrin ring^{28,29} and the d_π orbitals of the metal can overlap to form

two low-energy molecular orbitals that are mainly porphyrin in character and are filled and two high-energy (valence) molecular orbitals that are mainly metal in character and contain three electrons.⁵ The odd electron in the higher-energy set gives rise to the spin delocalization that results in the observed contact shift pattern,^{5,7} and it is to the hole in this orbital that the electron is added upon reduction of Fe(III) to Fe(II). We have recently shown⁵ that a heme substituent that is strongly electron-donating or -withdrawing relative to the others can cause significant redistribution of unpaired electron spin density around the porphyrin ring, due to the readjustment of orbital coefficients within the valence e(π) MOs. Such substituent effects are typically expected to cause splitting, ΔE_π , of the formerly degenerate valence e(π) orbitals shown in Figure 1 by only small amounts,^{5,7} and thus both orbitals are utilized for spin delocalization to a significant extent as the temperature is varied, according to their nearly equal but varying Boltzmann populations.

[⊗] Abstract published in *Advance ACS Abstracts*, November 15, 1995.

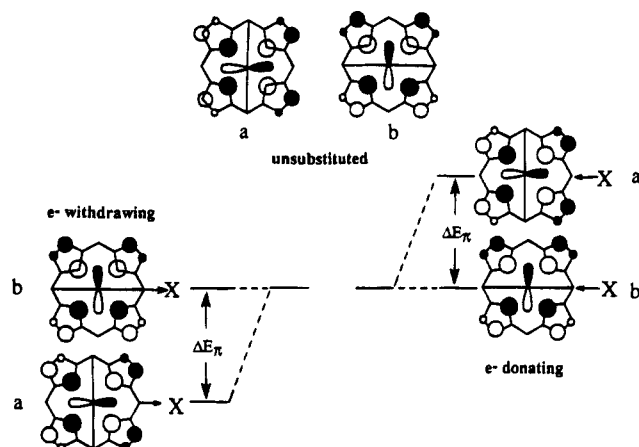


Figure 1. Formation of molecular orbitals by the interaction of the porphyrin $3e(\pi)$ orbitals²⁸ and the d_x metal orbitals produces a low-energy $e(\pi)$ bonding MO set that is mainly porphyrin in character and is completely filled and a higher energy (valence) “antibonding” MO set that is mainly metal in character and contains three electrons. Only the higher energy “antibonding” valence set is shown in the center of the figure. For a symmetrically substituted porphyrin, $X = Y$, the two e -symmetry valence orbitals are degenerate. By having placed the nodal planes at the *meso* positions, as required by the symmetry of (tetraphenylporphyrinato)iron(III) complexes, the electron density distribution is seen to be large—small within each pyrrole ring, or $\rho_{Ca} = \rho_{Cd} \gg \rho_{Cb} = \rho_{Cc}$ for the valence orbital derived from that shown in (a) and $\rho_{Ca} = \rho_{Cd} \ll \rho_{Cb} = \rho_{Cc}$ for the valence orbital derived from that shown in (b). If the symmetry of the system is lowered by introducing one unique *meso* substituent ($X \neq Y$), the two e -symmetry valence molecular orbitals will no longer be degenerate, and their electron density distribution will be modified slightly by the electron-donating/withdrawing characteristics of the unique substituent, and the energy degeneracy will be lifted. The effect of this lifting of degeneracy will determine which orbital is preferred for unpaired electron spin delocalization. A planar axial ligand can likewise lift the degeneracy of the $e(\pi)$ orbitals; the nodal plane of the ligand will define the orientation of the nodal plane of the $e(\pi)$ orbital preferred for spin delocalization. If the nodal plane of the ligand is misaligned with that of the unique *meso* substituent, then all eight pyrrole carbons will have uniquely different spin densities.

On the other hand, a planar axial ligand that is prevented from rotation by specially designed model compounds^{5–8} or by hydrogen bonding of a histidine or crowding of a methionine ligand within the binding pocket of a heme protein can enforce a relatively large energy difference ΔE_π between the two valence $e(\pi)$ molecular orbitals of the heme. Our earlier estimates, based upon EPR g values,⁸ suggested that for bis(imidazole)-coordinated ferriheme centers the maximum splitting, in that case called “ V ”, could be 2λ (where λ is the spin–orbit coupling constant for low-spin Fe(III); $\lambda = 300\text{--}400\text{ cm}^{-1}$, depending on assumptions). Since the electron that is added upon reduction of Fe(III) to Fe(II) will go into the higher energy of these two valence $e(\pi)$ molecular orbitals, the reduction potentials of model hemes and heme proteins may be modulated by the relative energies of the two valence $e(\pi)$ molecular orbitals.^{8,30} In considering the consequences of a relatively large value of ΔE_π (relative to $k_B T$), we will show that the temperature dependence of the contact shifts of some pyrrole substituent resonances of model hemes or heme proteins may show “anti-Curie” behavior (increasing magnitude of isotropic shift with increasing temperature), while the contact shifts of other pyrrole substituent protons in the same molecules show “Curie” behavior (decreasing magnitude of isotropic shift with increasing temperature). “Anti-Curie” behavior has been reported for two of the heme methyl resonances of cytochrome c_H ,¹⁸ where the axial methionine π -symmetry lone pair orientation is believed to be the important factor in determining ΔE_π , and for *Aplysia*

cyanometmyoglobin¹⁵ and cytochromes b_5 ,²² where the histidine imidazole plane(s) is/are the factor that determines ΔE_π . Even if ΔE_π is not large enough for “anti-Curie” dependence to be observed, we will see that the orientation of the filled π -symmetry lone pair of either methionine or histidine is responsible for the large spread of the heme β -pyrrole substituent resonances of both model hemes and heme proteins, as well as for the nonzero isotropic shifts at infinite temperature.

Model Development

General Comments. Many paramagnetic systems display well-established Curie behavior of their isotropic shifts, *i.e.*, linear dependence with inverse temperature. The obvious explanation of this is that the energy structure of paramagnetic compounds usually consists of well-separated (in the scale of thermal energy, $k_B T$) levels. These levels may be different electron multiplets or Kramers doublets, in the case of large spin–orbit interaction. The case of a small zero-field splitting (in comparison with $k_B T$) can also be included in this scheme if closely spaced energy levels are treated as a single level. In such cases the ground state can be considered as an isolated electronic level with small splitting of sublevels, $\Delta E_{\text{sublevels}} \ll k_B T$. The isotropic shifts for this level can be found by averaging over spin projections and molecular orientations of the paramagnetic contribution to the spin Hamiltonian.³¹ There are two mechanisms of influence of the paramagnetic center on the nuclei with which they interact: The contact or Fermi contribution

$$\hat{H}_{\text{HFI}}(\hat{S}, \hat{I}) = \vec{S} \cdot \vec{A} \vec{I} \quad (1)$$

and the dipolar or pseudocontact contribution

$$\hat{H}_{\text{dip}}(\hat{S}, \hat{I}) = \frac{\vec{\mu}_e \vec{\mu}_N}{R^3} - \frac{3(\vec{\mu}_e \vec{R})(\vec{\mu}_N \vec{R})}{R^5} \quad (2)$$

where \vec{R} is the vector connecting the NMR-active nucleus to the metal center and all other symbols have their conventional meanings.

The expressions for NMR isotropic shifts may be slightly different depending upon possible assumptions about the relative values of electron spin relaxation rates, transition frequencies, and rotational correlation times. However, all these expressions predict linear dependence of isotropic shifts with inverse temperature, the Curie law:

$$\delta = F/T \quad (3)$$

where F is the Curie factor. The inverse temperature dependence in eq 3 simply expresses the fact that it is sufficient to take into account only the first-order terms in the expansion of the Boltzmann factors $\exp(-\Delta E_{\text{sublevels}}/k_B T)$. (However, in some cases it may be necessary to consider the second-order Zeeman contributions.³²) The constant F is determined by the properties of the molecule and in both mechanisms can be either positive or negative. For the case of a pure spin state the following expressions are usually used:⁷

$$\delta_{\text{con}} = \frac{A\beta g S(S+1)}{\gamma_N \hbar 3k_B T} \quad (4)$$

and

$$\delta_{\text{dip}} = \frac{1}{3} \left\{ \left[\chi_{zz} - \frac{1}{2}(\chi_{xx} + \chi_{yy}) \right] [3 \cos^2 \Theta - 1] + \frac{3}{2}(\chi_{xx} - \chi_{yy}) \sin^2 \Theta \cos 2\Phi \right\} r^{-3} \quad (5)$$

where R , Θ , and Φ are the polar coordinates of the nucleus relative to the paramagnetic center and the principal values of χ can be calculated (to second order if desired³²) from the EPR g values using Van Vleck's equation. For bis(imidazole)-coordinated ferrihemes, however, second-order Zeeman corrections have been shown to be negligible,³² and therefore g values could be used to calculate the axial and rhombic contributions to the dipolar shift. The sign of the contact shift is determined by the hyperfine coupling constant A , which is positive for direct spin delocalization through π orbitals and negative for spin-polarization mechanisms involving penetration of spin density to the nucleus, such as those involved with delocalization through σ bonds. The sign of the dipolar shift is determined by both geometric factors and the orientation of the principal axes and values of the χ tensor.

Multilevel Case. In some systems, deviations of the temperature dependence of the isotropic shift from the simple Curie law (eq 3) have been observed.^{3,6,7,11,13,15,33} These deviations can be understood by considering the presence of low-lying excited states where the differences in energy between ground and excited levels are of the order of the thermal energy, $k_B T$. In this case, as pointed out previously,³² the thermal population of the excited states must be taken into account. This is easily done by averaging the equations for the isotropic shifts with their Boltzmann weighting factors. Let $\delta_{n,l}$ be the isotropic shift of nucleus n in a pure electronic state l . The observable shift of nucleus n is then

$$\delta_n = (1/Z) \sum_l \delta_{n,l} W_l e^{-E_l/k_B T} \quad (6)$$

where Z is the statistical sum,

$$Z = \sum_l W_l e^{-E_l/k_B T} \quad (7)$$

and W_l is the statistical weight of the state l ; $W_l = 2S_l + 1$ for a pure spin state.

In eq 6 isotropic shifts $\delta_{n,l}$ of nucleus n for any level l obey the Curie law (3), and eqs 6 and 7 can be considered to result from two step averaging: (i) averaging over sublevels within level l and (ii) averaging over all levels l .

Analysis of the Two-Level Case. For most real systems it is unlikely that more than two levels are within thermal energy of the ground state. Even the case of two relatively closely spaced levels is quite rare. The typical origin of the two-level case is the splitting of formerly degenerate electronic states due to unsymmetrical perturbations (e.g., unsymmetrically placed substituents or a planar axial ligand). The spin-admixed ($S = 3/2, 5/2$) ground state of cytochromes c' and PorFeOClO_3 systems is also a case that is likely to have low-lying excited states.³⁴⁻³⁹ In fact, the proximity of the $S = 3/2$ and $S = 5/2$ states is the necessary condition for the existence of admixed spin states; the former pure states are mixed and split by the spin-orbit interaction.

In these two-level cases the general expressions 6 and 7 reduce to the following:

$$\delta_n = \frac{1}{T} \frac{W_1 F_{n,1} + W_2 F_{n,2} e^{-T^*/T}}{W_1 + W_2 e^{-T^*/T}}, \quad T^* = (E_2 - E_1)/k_B \quad (8)$$

At high temperatures the dependence of δ_n on $(1/T)$ tends toward a straight line with the average slope of the ground and excited state:

$$\delta_n \rightarrow \frac{1}{T} \frac{W_1 F_{n,1} + W_2 F_{n,2}}{W_1 + W_2} + \frac{T^*}{T^2} \frac{W_1 W_2 (F_{n,2} - F_{n,1})}{(W_1 + W_2)^2}, \quad T \gg T^* \quad (9)$$

At low temperatures (but still within the condition that $\Delta E_{\text{sublevels}} \ll k_B T$) the temperature dependence of the isotropic shifts is mainly determined by the ground state.

$$\delta_n \approx \frac{F_{n,1}}{T} + \frac{W_2}{W_1 T} (F_{n,2} - F_{n,1}) e^{-T^*/T}, \quad T \ll T^* \quad (10)$$

Between these two extreme straight line limits the dependence $\delta_n(1/T)$ deviates, in general, from the Curie law (except for the case $F_{n,1} = F_{n,2}$). The next order corrections to the above extreme linear dependencies are also presented in eqs 9 and 10. If eq 8 is rewritten as a product of a constant factor (the isotropic shift of the excited state at temperature T^*) and a universal function ϕ :

$$\delta_n(T) = \delta_{n,2}(T^*) \phi(x, \kappa, \omega), \quad \phi(x, \kappa, \omega) = x \frac{\kappa \omega + e^{-x}}{\omega + e^{-x}}, \quad x = \frac{T^*}{T} \quad (11)$$

Here $\kappa_n = \delta_{n,1}/\delta_{n,2} = F_{n,1}/F_{n,2}$, $\omega = W_1/W_2$, and both parameters are independent of temperature. Note that $\delta_{n,2}(T^*)$ can be recalculated at any temperature using the relation $\delta_{n,2}(T)T = \delta_{n,2}(T^*)T^*$. The function $\phi(x)$ for different κ but the same ω has an inflection point at the same position $x_i(\omega)$, determined by the equation

$$\omega \exp(x_i) = (x_i + 2)/(x_i - 2) \quad (12)$$

where $x_i(1) = 2.3994$, $x_i(6/4) = 2.2897$, and $x_i(4/6) = 2.5379$. The shape of the function $\phi(x)$ (and the form of the temperature dependence of the isotropic shift in a two-level system) depends mainly on κ . Only at $\kappa = 1$ (the same Curie factors F for the ground and excited states) does eq 11 reduce to the Curie law. For any other κ eq 11 predicts deviations from Curie dependence, but for $\kappa > \kappa_b(\omega)$ this dependence is at least monotonic: The larger the value of x (or $1/T$), the larger the absolute value of the observed isotropic shift. The boundary value of κ depends on the ratio of the statistical weights: $\kappa_b(1) = 0.0908$, $\kappa_b(6/4) = 0.0675$, and $\kappa_b(4/6) = 0.1185$. At finite experimental temperature intervals this dependence still looks like the Curie law (but with the wrong high-temperature limit ($x = 0$)).

For $\kappa < \kappa_b$ there is a region of "anti-Curie" behavior. More precisely, this is the region where the absolute value of the isotropic shift decreases with increasing inverse temperature. The interval of "anti-Curie" behavior spreads in both directions with decrease of κ . At $\kappa = 0$ (no isotropic shifts in the ground state) this interval begins at $x = 1.2785$ (for $\omega = 1$) and extends to infinity. (For $\kappa = 0$ and $\omega = 6/4$ the left boundary is 1.2066, and for $\omega = 4/6$ it is 1.3781.) For negative values of κ (different signs of the shifts for the ground and excited state), the left boundary shifts to the left, but at a certain temperature the observed chemical shift changes its sign, and the magnitude increases with increasing inverse temperature. All these types of behavior are shown in Figure 2.

Conditions for the Existence of "Curie" and "Anti-Curie" Behavior. In principle, both the contact and dipolar mecha-

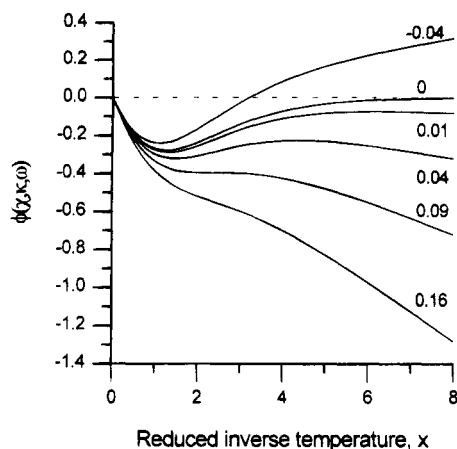


Figure 2. Dependence of the two-level fitting function $\phi(x, \kappa, \omega)$, eq 11, on reduced inverse temperature, $x = T^*/T$ for different ratios of Curie factors $\kappa = F_1/F_2$ and $\omega = W_1/W_2 = 1$. The lines correspond to the behavior for the ratios c_1^2/c_2^2 listed.

nisms allow nonlinear temperature dependence and even “anti-Curie” behavior, as was anticipated in the pioneering work of Horrocks and Greenberg.³² In the dipolar mechanism the \mathbf{g} tensor and thus χ values for different states may have different anisotropy and magnitude of the g values (see eq 5). For example, if the ground state has an almost isotropic \mathbf{g} tensor while the excited state has considerable anisotropy, then the conditions for “anti-Curie” behavior can be satisfied. The existence of both “Curie” and “anti-Curie” behavior for different nuclei in the same molecule is more unlikely because the two states have the same geometric factors, and this complex behavior requires very specific combinations of the three g values. However, the possibility remains of the existence of different directions of principal axes (relative to which the angles Θ and Φ are calculated) in the two states. For ground and excited states that involve a hole in one of the d_{π} orbitals, either d_{yz} or d_{xz} , such as those represented by the low-spin Fe(III) hemes of interest to this study, population of the excited state corresponds to a change in sign of the rhombic dipolar term but no change in the axial dipolar term. Thermal population of the excited state will thus result in a rotation (or twisting) of the axes of the in-plane magnetic anisotropy, as has frequently been observed for heme proteins,^{21k-m,22a,f} and a diminution in its magnitude. It should be noted, however, that, except for these cases, these intuitive conclusions often cannot be verified because of the lack of data on the magnetic properties of the excited states in comparison to the ground states of metal complexes.

The conditions for “anti-Curie” dependence, and especially the presence of the two types of dependences in one molecule, are easier to achieve for the contact contribution to the isotropic shifts. Although either σ or π delocalization could be involved, this is especially true in the case where the unpaired electron is delocalized into a π -symmetry orbital of the ligand. Let us introduce into eq 4 the McConnell relation between the hyperfine constant of a proton A_H and the π -electron spin density at a carbon atom ρ_C to which a hydrogen is attached.⁴⁰ Then for the nucleus n in the state i we have

$$\delta_{n,i} = \frac{\beta g(S+1)QC_{n,i}^2}{\gamma_H \hbar 6k_B T} = \frac{fC_{n,i}^2}{T} \quad (13)$$

$$A_H = Q\rho_C/2S \quad (14)$$

Here we have expressed the spin density in terms of the

coefficient of the molecular orbital (MO) that contains the unpaired electron $\rho_{ni} = C_{ni}^2$. (In the general case it is necessary to sum over all half-filled MOs.) For $Q = -63$ MHz the factor $f = -4.968 \times 10^5$ ppm K. Quantum-chemical calculations with different levels of approximations (ranging from simple and extended Hückel to *ab initio*) show that for a given MO the coefficients may vary by factors of ~ 2 – 5 and, consequently, the densities by almost an order of magnitude, since they are the squares of the coefficients. Moreover, there may be very small spin densities for one or the other orbital, if atoms are near or at the nodal plane of the MO.

The most important factor for the existence of the two types of temperature dependences in the same molecule is that the MOs of the ground and excited states may have quite different shapes, *e.g.*, different orientation of the nodal planes. Such a situation makes possible the existence of different values of κ for the different nuclei, which can satisfy either “Curie” or “anti-Curie” behavior, if the energy separation between the ground and excited states, $E_2 - E_1 = \Delta E$, is large compared to $k_B T$ at room temperature, as we will show below.

The Possibility of Extraction of Molecular Information from NMR Data. *Method.* We have applied the least-squares method for the determination of the properties of the ground and excited state. That is, we have minimized the sum of the squares of deviations of the observed and theoretical isotropic shifts for all NMR lines at all temperatures with respect to $2N + 1$ parameters $F_{n,1}$, $F_{n,2}$, and T^* .

$$\sigma^2 = \frac{1}{MN} \sum_{m=1}^M \sum_{n=1}^N [\delta_n(T_m; F_{n,1}, F_{n,2}, T^*) - \delta_n^{\text{exp}}(T_m)]^2 w_m^n \quad (15)$$

In eq 15 N is the number of NMR lines, M is the number of temperature points, and the theoretical dependence of the isotropic shifts is given by eq 8. The accuracy of the measurements is taken into account by the weights w_m^n . Usually, experimental errors are assumed to obey the normal distribution with standard deviations σ_{nm} . In this case the weights should be taken to be inversely proportional to the variances: $w_m^n = 1/\sigma_{nm}^2$. If there is no available estimate of the accuracy, equal weights ($w_m^n = 1$) should be taken.

The solution of this problem can be achieved in two steps: (i) minimization of σ^2 with respect to linear parameters $F_{n,1}$, and $F_{n,2}$; (ii) minimization with respect to the energy gap ΔE between the levels (or T^*).

The first step splits into N independent 2 by 2 problems:

$$\begin{pmatrix} \langle \vec{P} \vec{P} \rangle & \langle \vec{P} \vec{Q} \rangle \\ \langle \vec{Q} \vec{P} \rangle & \langle \vec{Q} \vec{Q} \rangle \end{pmatrix} \cdot \begin{pmatrix} F_{n,1} \\ F_{n,2} \end{pmatrix} = \begin{pmatrix} \langle \vec{P} \vec{\delta}_n \rangle \\ \langle \vec{Q} \vec{\delta}_n \rangle \end{pmatrix} \quad (16)$$

where $\vec{\delta}_n$ is the vector of the experimental isotropic shift of nucleus n at M temperature points; and \vec{P} and \vec{Q} are M -dimensional vectors with the following components:

$$P_m = \frac{1}{T_m} \frac{W_1}{W_1 + W_2 \exp\left(-\frac{T^*}{T_m}\right)} \quad Q_m = \frac{1}{T_m} \frac{W_2}{W_2 + W_1 \exp\left(\frac{T^*}{T_m}\right)} \quad (17)$$

Here brackets denote the weighted scalar product of the M -dimensional vectors:

$$\langle \vec{A} \vec{B} \rangle = \sum_{m=1}^M A_m B_m w_m \quad (18)$$

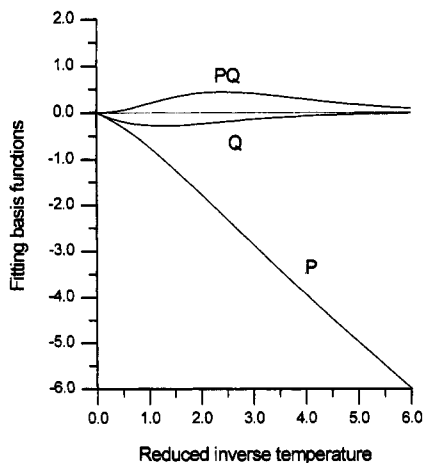


Figure 3. Plot of two-level fitting basis functions P and Q , corresponding to basis vectors (17). The best fit of the temperature dependence of isotropic shifts is a linear combination (19) of P and Q . The change in the temperature dependence due to variation of the energy gap is proportional to PQ (eq 20).

The solution of eqs 16–18 provides the best presentation of experimental shifts with the given vectors \vec{P} and \vec{Q} :

$$\vec{\delta}_n \approx F_{n,1} \vec{P} + F_{n,2} \vec{Q} \quad (19)$$

In other words, the right hand side of eq 19 is the vector that represents the most probable value of the experimental isotropic shifts.

The second step, the minimization of the mean-square deviation σ (eq 15) with respect to the only nonlinear parameter T^* , should be performed numerically using any of the usual methods for one dimensional minimization.^{41,42} During the minimization, a change in T^* alters the form of vectors \vec{P} and \vec{Q} according to eq 17. To a first approximation, this reduces to the additional vector $\Delta T^* \vec{R}_n$ on the right-hand side of eq 19, with the following components

$$(\vec{R}_n)_m = (F_{n,1} - F_{n,2}) P_m Q_m \quad (20)$$

The dependence of the universal basis functions P , Q , and PQ , corresponding to vectors (18,20), upon the reduced inverse temperature T^*/T is presented in Figure 3.

Accuracy and Stability. In the processing of experimental data, the most important questions are the accuracy of the extracted values and the stability of the processing procedure. The stability of the first stage with respect to round-off and experimental errors can be characterized by the parameter ρ , which is defined as the square root of the ratio of the largest and smallest eigenvalues of the matrix in eq 16.⁴² In other words, ρ is the ratio of singular values of the two-column matrix consisting of the vectors \vec{P} and \vec{Q} and the smaller the value of ρ , the more stable the procedure is. The minimal value of ρ can be 1, but a value of $\rho < 10^2$ is appropriate.⁴² For the case of matrix (16), the eigenvalues are

$$r_{1,2} = (\langle \vec{P} \vec{P} \rangle + \langle \vec{Q} \vec{Q} \rangle) \pm \sqrt{(\langle \vec{P} \vec{P} \rangle - \langle \vec{Q} \vec{Q} \rangle)^2 + 4 \langle \vec{P} \vec{Q} \rangle^2} / 2 \quad (21)$$

$$\rho = \sqrt{r_1/r_2}$$

The parameter ρ is mainly determined by the interval of the measurements and does not depend on the form of the temperature dependence of the isotropic shifts. More precisely, it is determined by the interval of the dimensionless inverse temperature $x = T^*/T$, and consequently, ρ depends indirectly

on the energy gap between states. For example, if for some excitation energy the interval for x is [1,3] and $\rho = 16.3$, then for half the energy the interval is [0.5,1.5] and $\rho = 13.1$, and for twice the energy the interval is [2,6] and $\rho = 45.4$.

The accuracy in the determination of Curie factors $F_{n,1}$ and $F_{n,2}$ depends on the accuracy and number of measurements. The expressions for their variances can be easily derived: If unit weights were used in eq 18, then the right-hand side of eq 22

$$\text{variance}(F_1) = \frac{\langle \vec{Q} \vec{Q} \rangle}{\langle \vec{P} \vec{P} \rangle \langle \vec{Q} \vec{Q} \rangle - \langle \vec{P} \vec{Q} \rangle^2} \quad (22)$$

$$\text{variance}(F_2) = \frac{\langle \vec{P} \vec{P} \rangle}{\langle \vec{P} \vec{P} \rangle \langle \vec{Q} \vec{Q} \rangle - \langle \vec{P} \vec{Q} \rangle^2}$$

should be multiplied by some estimation of the variance of the experimental errors. Equations 22 predict that variances for the coefficients $F_{n,1}$ and $F_{n,2}$ are directly proportional to the variance of errors and inversely proportional to the number of measurements N . Note that the numerator for F_2 is larger than that for F_1 . This means that the properties of the excited state are less accurately determined than those of the ground state. For the interval $1 < x < 3$ and $\omega = 1$, the ratio $\sqrt{\langle \vec{P} \vec{P} \rangle / \langle \vec{Q} \vec{Q} \rangle} = 8.1$. All these parameters, characterizing the accuracy of the reconstruction of the Curie factors $F_{n,1}$ and $F_{n,2}$, can be easily calculated together with the solution of eq 16.

In contrast to the first stage, the accuracy in determination of the energy gap (or T^*) depends mainly on the form of the temperature dependence of the isotropic shifts. As an example, consider the case of one line with a pure linear dependence of isotropic shift upon inverse temperature (Curie behavior). In this case eq 16 provides equal Curie factors for both states, but the mean-square deviation σ (15) does not depend on the excitation energy, and there is an infinite uncertainty in its determination. Thus, the main reason for the simultaneous processing of several NMR lines is the increased reliability of the results, especially the energy gap, ΔE . Unfortunately, it is difficult to present the estimation of the accuracy of T^* in a closed form, but it can be done numerically during the minimization with respect to excitation energy. The uncertainty in ΔE can be estimated as follows:

$$\text{variance}(\Delta E) = 2\sigma^2 / \left(\frac{\partial^2 \sigma^2}{\partial \Delta E^2} \right) \quad (23)$$

This means that the deviation of σ^2 from its minimum value is of the order of σ^2 if ΔE differs from its optimal value by the standard deviation, corresponding to eq 23.

Numerical Experiments. The above considerations were tested by the following numerical experiments. The contact interaction only was considered, and the chemical shifts were calculated using eqs 14 and 8 with $W_1 = W_2$. The energy gap was taken as 350 cm^{-1} or $T^* = 503.6 \text{ K}$. The spin densities for the ground and excited states, corresponding to four NMR lines, listed in Table 1, were used. The inverse temperature points $x = 1000/T$ were taken equally spaced with step 0.2 in the interval $2.6 \leq x \leq 5.4$. It was assumed that the main source of errors is the temperature instability during the NMR measurements. Experimental noise was modelled according to the relation

$$\Delta \delta_n = \frac{d\delta_n(x)}{dx} \frac{dx}{dT} \Delta T \propto \frac{d\delta_n}{dx} \frac{\Delta T}{T^2} \quad (24)$$

For ΔT the normal random values with standard deviations of

TABLE 1: Spin Densities Used for Model Calculations

proton	C_{ground}^2	C_{excited}^2
a	0.000 600	0.016 000
b	0.016 000	0.000 600
c	0.020 000	0.000 400
d	0.000 400	0.020 000

TABLE 2: Results of Reconstruction of the Numerical Experiments

(a) variance (ΔT) = 1 K, $\sigma^2 = 0.007$, $T^* = 492.6$ K			(b) variance (ΔT) = 3 K, $\sigma^2 = 0.07$, $T^* = 470.5$ K		
proton	C_{ground}^2	C_{excited}^2	proton	C_{ground}^2	C_{excited}^2
a	0.000 544	0.015 845	a	0.000 422	0.015 560
b	0.016 083	0.000 589	b	0.016 266	0.000 540
c	0.0200 31	0.000 772	c	0.020 099	0.001 473
d	0.000329	0.019 797	d	0.000 175	0.0194 26

1 or 3 K were used. According to eq 22, the standard deviations of $\Delta\delta$ are proportional to the square of the inverse temperature x . If the derivatives $d\delta_n/dx$ are approximately constant in the temperature interval of the NMR measurements, then the optimal weights in eqs 15 and 18 should be taken as inversely proportional to the variances or inverse to the fourth power of x :

$$w_m \propto x_m^{-4} \quad (25)$$

The results of the reconstruction of such numerical experiments are presented in Table 2. The errors of the reconstructed values depend on the amount of noise and may be either negative or positive. In the above examples we assumed the same noise, but different variances. In the first case the accuracy in the excitation energy is about 2.2% and in the second about 6.6%. The absolute errors in spin densities for the ground and the excited states for the two cases are 0.000 06, 0.0002 and 0.000 17, 0.0004, respectively. The ratios of errors excited/ground roughly correspond to the estimated value 5, according to eq 22. It was also found that eq 21 overestimates the error in energy, and instead of a factor of 2 one should take a factor of 10 less.

The processing of the same model data with equal weights gives slightly less accuracy. For the two cases, the accuracy in the reconstruction of energies is 3.1% and 8.4%, and corresponding increases in errors in spin densities are observed.

Analysis of Experimental Data: Low-Spin Fe(III) Model Hemes and Heme Proteins. In most low-spin iron(III) porphyrinates, the $e(\pi)$ valence molecular orbitals shown in Figure 1 are believed to be responsible for spin delocalization to the protons on the periphery of the porphyrinate ligand. Of the large number of temperature dependences of the isotropic shifts of such systems reported thus far, we have analyzed the contact part of the shifts observed in some of these systems according to eq 8 utilizing the fitting procedures described above. In order to estimate the dipolar contribution to the isotropic shifts of tetraphenylporphyrinates, we have calculated the axial dipolar shift of the pyrrole-H from the m -H isotropic shift at a particular temperature, scaled to the relative geometric factors for the m -H and pyrrole-H positions, and then again scaled to the absolute temperature of each data point, as outlined previously.⁷ (It should be noted that this procedure does not work for low-spin ferriheme complexes having other axial ligands, such as cyanide, that have measurable unpaired electron spin density at the *meso* carbons and their substituents.³³) The axial dipolar shifts were then subtracted from the observed isotropic shifts. No correction was made for the rhombic dipolar shifts of the systems having freely rotating axial ligands because (i) it was found that this term did not affect the value of ΔE_π

obtained from the fits and (ii) we believe that the rhombic or in-plane magnetic anisotropy is extremely small or zero in such systems. For systems having hindered axial ligand rotation or fixed orientations of axial ligands, the rhombic contributions to the dipolar shift were also not calculated for the reasons discussed below.

Unsymmetrically Substituted Low-Spin Fe(III) Model Hemes. The Curie plots of a number of complexes of the type $[(X)_3-(Y)_1\text{TPPF}e(\text{NMeIm})_2]\text{Cl}$, where $X \neq Y$ are substituents on the phenyl rings of the tetraphenylporphyrinate, have been reported previously.^{3,11} In each of the Curie plots, nonzero intercepts of the individual proton temperature dependence lines were observed, and in most cases, the lines crossed each other at $1000/T \sim 1.5-2 \text{ K}^{-1}$.^{3,11} In spite of the individual deviations, in most cases the *average* temperature dependence of the resonances appeared to strictly obey the Curie law. Detailed analysis of the observed nonzero intercepts indicated that the spread of the intercepts of individual lines correlated with the difference in electron-withdrawing or -donating properties of the substituents X and Y , as measured by the Hammett σ constants of the substituents.³ The reason for the crossing of the lines at $1000/T \sim 1.5-2.0 \text{ K}^{-1}$ was at that time not known, since the second-order Zeeman contribution to bis(imidazole)-coordinated hemins has been shown to be very small.³² However, this crossing can now be explained on the basis of the present work as being due to the linear fitting of the NMR data for a system in which there are two thermally accessible energy levels that are separated by an energy ΔE_π , where ΔE_π may be relatively small. For most of the data reported in ref 3, for which NMR spectra of substituted model hemins having freely rotating axial ligands were recorded in CDCl_3 to -65°C , in most cases ΔE_π was found to be too small to estimate. Isotropic shifts obtained above $\sim 0^\circ\text{C}$ were found to be affected by chemical exchange between the low-spin bis(*N*-methylimidazole) complex and its high-spin mono-ligand counterpart, formed by dissociation of one axial ligand.^{11,43} Therefore, isotropic shift data obtained above 0°C could not be used for analysis according to the methods described above. Thus, the number of data points that could be used was severely limited, and attempts to fit the data of many of the complexes led to errors that were larger than the magnitude of ΔE_π . For the two formula isomers, $[(p\text{-Cl})_3(p\text{-NEt}_2)\text{TPPF}e(\text{N-MeIm})_2]^+$ and $[(p\text{-NEt}_2)_3(p\text{-Cl})\text{TPPF}e(\text{N-MeIm})_2]^+$, linear (one-level with forced equal intercepts for all signals) analysis according to eq 8 provided acceptable fits, as shown in Figure 4, a and b, respectively, with small nonzero intercepts, indicating that ΔE_π is very small. Two-level fitting indicated very little dependence of the quality of fit on the value of ΔE_π and hence an inability to reliably estimate its value. For the complex $[(o\text{-NO}_2)_1\text{TPPF}e(\text{N-MeIm})_2]^+$ (which may in fact have some hindrance to ligand rotation due to the *ortho*-nitro substituent on one phenyl ring), for which isotropic shifts were measured in CD_2Cl_2 to -90°C ,¹¹ fitting the data obtained below 0°C to eq 8 leads to the plot shown in Figure 5, an estimate of ΔE_π of 77 cm^{-1} ($\pm 47 \text{ cm}^{-1}$), and quantitatively reasonable spin density coefficients ρ for ground and excited state orbitals (caption to Figure 5). If instead this system is treated as having only one energy level ($\Delta E_\pi = 0$), the predicted diamagnetic shift is 8.08 ppm, while the known diamagnetic shift of the pyrrole-H of the free base porphyrin is approximately 8.9 ppm. In all of the fits for systems having small values of ΔE_π , the values obtained from the fitting procedure are extremely sensitive to the number and quality of data points.

Model Heme Complexes Having at Least One Planar Axial Ligand That Is Hindered in Rotation. We have recently reported

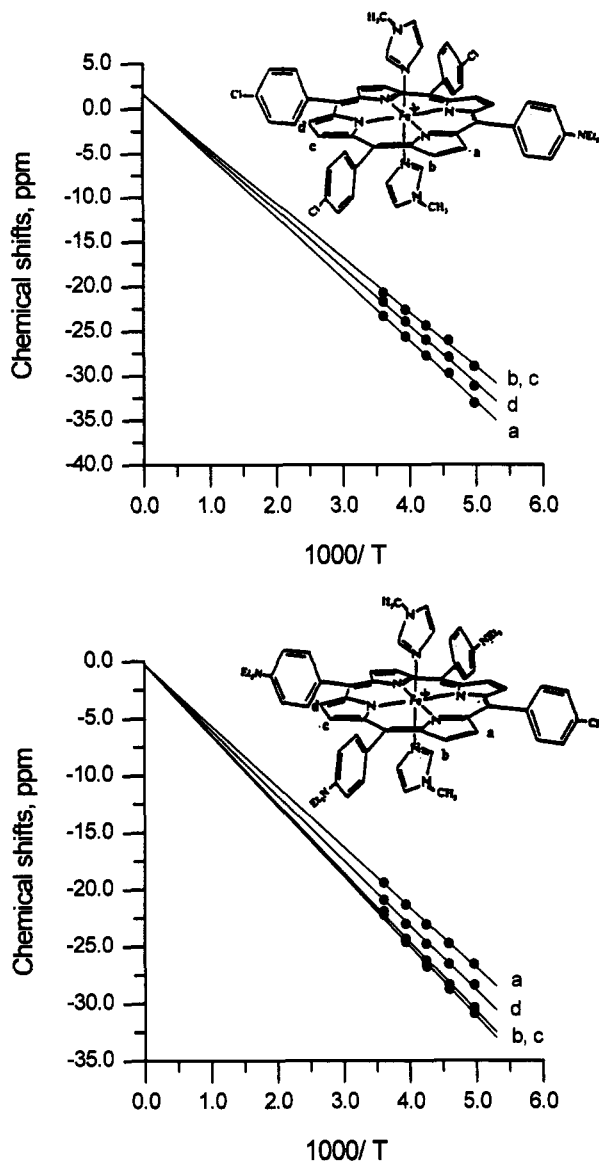


Figure 4. One-level plots of eq 8 (assuming ΔE_π to be zero) to the calculated contact shifts of the pyrrole-H of (a, top) $[(p\text{-Cl})_3(p\text{-NEt}_2)_2]\text{TPPFe}(N\text{-MeIm})_2^+$ and (b, bottom) $[(p\text{-NEt}_2)_3(p\text{-Cl})_2]\text{TPPFe}(N\text{-MeIm})_2^+$.³ Spin density coefficients, ρ_c , obtained from this one-level fitting procedure are as follows: for the first complex, (a) 0.0139, (b, c) 0.0123, (d) 0.0131; for the second, (a) 0.0107, (b) 0.0122, (c) 0.0124, (d) 0.0115. The two-level fits to eq 8 are not acceptably better than these, indicating that ΔE_π is very small.

a detailed ^1H NMR study of several novel oxomolybdenum(V)-appended low-spin Fe(III) porphyrins.¹² It was observed that the Curie plots, while appearing to be linear, show relatively large nonzero intercepts, and the two sets of up to eight resolved pyrrole-H resonances cross each other at $1000/T \sim 1.5\text{--}2.0\text{ K}^{-1}$ for two of the three complexes. (The data for the complex in which the axial ligands are imidazole are less easily understood, since there is a high probability that hydrogen bonding of the imidazole N-H proton to the chloride anion⁴⁴ has a major influence on both the observed isotropic shifts and their temperature dependence.)

In order to analyze the temperature dependence of these spectra, it was necessary to determine how the rhombic dipolar term would behave in systems having a thermally accessible excited state. For these low-spin Fe(III) systems, population of the excited state corresponds to a change in sign of the rhombic dipolar term but no change for the axial dipolar term. Thermal population of the excited state thus results in a rotation

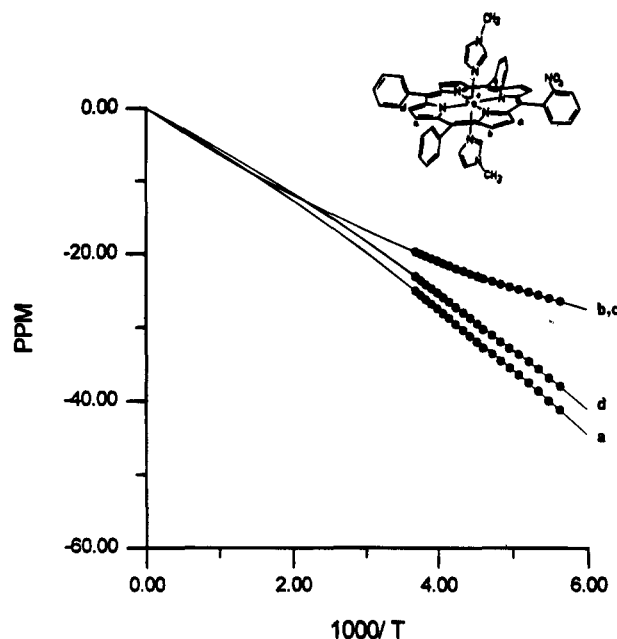


Figure 5. Plot of the fit of eq 8 to the calculated contact shifts of the pyrrole-H of $[(o\text{-NO}_2)_2]\text{TPPFe}(N\text{-MeIm})_2^+$.¹¹ The value of ΔE_π obtained from this fit is $77 \pm 47\text{ cm}^{-1}$, a relatively small value. Spin density coefficients obtained from this fit are, for the ground state, (a) 0.0193, (b, c) 0.0044, and (d) 0.0179, while for the excited state they are (a) 0.0022, (b, c) 0.0213, and (d) 0.0018. These values compare favorably with the magnitudes of those obtained from simple Hückel calculations [ground state: (a) 0.0173, (b, c) 0.0010, (d) 0.0162; excited state, (a) 0.0008, (b, c) 0.0176, (d) 0.0008].

of the average axes of the in-plane (rhombic) magnetic anisotropy and a diminution of its magnitude. Because the reversal in sign of the rhombic dipolar shift mimics the change in shape of the π molecular orbital that gives rise to the contact shift, and because the magnitude of the rhombic dipolar term is so much smaller than the contract contribution,¹² we have carried out the fitting procedures on the combined contact and rhombic dipolar shifts for the systems having fixed axial ligand planes, whether they be model hemes or heme proteins. The unpaired electron spin density coefficients obtained and listed in the figure captions therefore contain a small contribution from the rhombic dipolar term. However, test calculations showed that although the coefficients were affected slightly, the value of ΔE_π obtained from the fitting procedure was unaffected by ignoring or including a correction for the rhombic dipolar shift at each β -pyrrole position.

For the Mo(V)-appended ferriheme complex with the best resolved pyrrole-H resonances, that with *N*-methylimidazole axial ligands,¹² fitting of the calculated contact shifts to eq 8 yields a value of ΔE_π of $214 \pm 45\text{ cm}^{-1}$ and very reasonable spin densities, ρ . Comparison of observed data points and the lines obtained from our fitting procedure is shown in Figure 6, and the spin densities obtained for the ground and excited state orbitals are listed in the caption of that figure. The value of ΔE_π obtained is intermediate in size, indicating that at least one axial ligand is held *relatively* rigidly in one orientation, but there is probably *some* freedom for libration around an average orientation. For the 4-(dimethylamino)pyridine complex, the fitting did not yield a unique solution; the apparent value of ΔE_π is much smaller in this case, possibly because the pyridine ligands are held in perpendicular planes.

For the case of a covalently attached axial ligand, $[(o\text{-NHCOCH}_2\text{CH}_2\text{Im})]\text{TPPFe}(N\text{-MeIm})_2^+$ in CDCl_3 solution,³ excluding data obtained above 0°C leads to the fit shown in Figure 7 and a value of ΔE_π of $310 \pm 115\text{ cm}^{-1}$, a somewhat larger

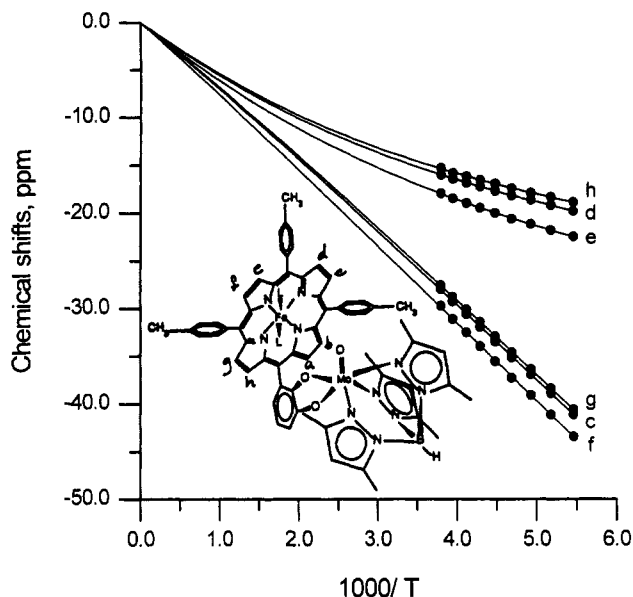


Figure 6. Plot of the fit of eq 8 to the calculated contact shifts of the pyrrole-H for $[(2,3\text{-Mo})\text{TPPFe}(\text{N-MeIm})_2]^+$.¹² The value of ΔE_π obtained from this fit is $211 \pm 25 \text{ cm}^{-1}$, an intermediate value. Spin density coefficients obtained from this fit are, for the ground state, (c) 0.0164, (d) 0.0059, (e) 0.0049, (f) 0.0158, (g) 0.0156, and (h) 0.0046, while for the excited state they are (c) 0.0141, (d) 0.0212, (e) 0.0199, (f) 0.0120, (g) 0.0114, and (h) 0.0195. These values compare reasonably with the magnitudes of those obtained from simple Hückel calculations.

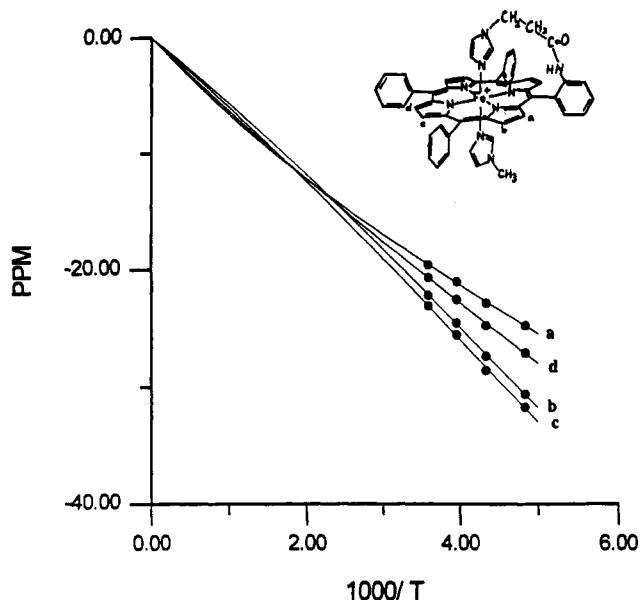


Figure 7. Plot of the fit of eq 8 to the calculated contact shifts of the pyrrole-H for $[(o\text{-NHCOCH}_2\text{CH}_2\text{Im})_1\text{TPPFe}(\text{N-MeIm})]^+$.³ The value of ΔE_π obtained from this fit is $310 \pm 115 \text{ cm}^{-1}$. Spin density coefficients obtained from this fit are, for the ground state, (a) 0.0135, (b) 0.0107, (c) 0.0092, and (d) 0.0131, while for the excited state they are (a) 0.0095, (b) 0.0157, (c) 0.0194, and (d) 0.0085. Again, these values compare favorably with the magnitudes of those obtained from simple Hückel calculations.

energy separation that indicates that one axial ligand is held *relatively* rigidly in orientation. Spin density coefficients for the ground and excited state orbitals obtained from this fit are listed in the caption to Figure 7 and are of similar magnitude to those obtained from molecular orbital calculations.

Heme Proteins Having at Least One Fixed Axial Histidine Plane. Peyton *et al.* have recently reported the temperature dependence of the heme resonances of *Aplysia* cyanometmyoglobin.¹⁵ We have estimated the axial dipolar term for the four

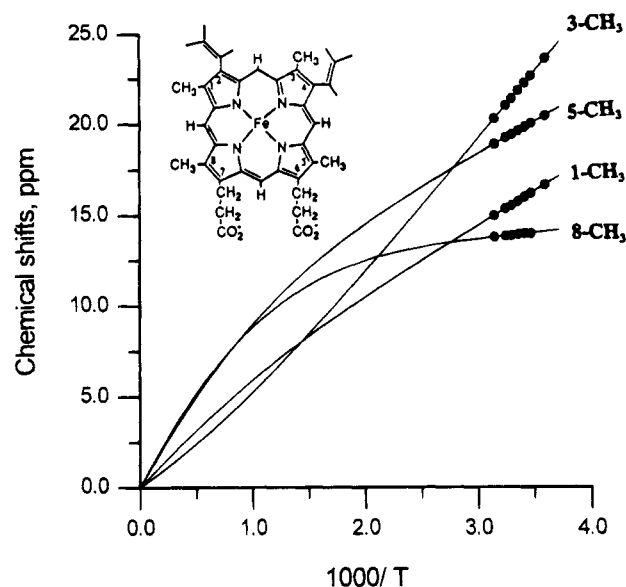


Figure 8. Plot of the fit of eq 8 to the experimental shifts of the four methyl resonances of *Aplysia* cyanometmyoglobin.¹⁵ The value of ΔE_π obtained from this fit is $498 \pm 53 \text{ cm}^{-1}$. This value compares favorably to that calculated from the g values of cyanometmyoglobin, $\Delta E_\pi = 313\text{--}368 \text{ cm}^{-1}$ (based upon the spin-orbit coupling constant, $\lambda \sim 340\text{--}400 \text{ cm}^{-1}$).^{8,32} For the ground state, the spin densities obtained from this fit are as follows: 1-Me, -0.0086 ; 3-Me, -0.0139 ; 5-Me, -0.0096 ; 8-Me, -0.0052 . For the excited state they are as follows: 1-Me, -0.0186 ; 3-Me, -0.0037 ; 5-Me, -0.0354 ; 8-Me, -0.0435 . These values compare reasonably with the magnitudes of those obtained from simple Hückel calculations.

heme methyl groups, 1-, 3-, 5-, and 8- CH_3 , from the reported g values of metMbCN⁴⁵ and the geometric factors of the methyl groups.³³ Again, as for the model hemes with a fixed axial ligand plane, we have not corrected for the rhombic dipolar shift. We have used the calculated axial dipolar shift, assuming that it follows the simple Curie law, to obtain the contact plus rhombic dipolar contributions to the isotropic shifts reported¹⁵ and have fit the temperature dependence of the four methyl groups to eq 8. We find that ΔE_π in this case is $498 \pm 53 \text{ cm}^{-1}$ ($\pm 11\%$), again with very reasonable spin densities, ρ , at the four methyl carbons (Figure 8 caption). Comparison of observed data and line fits for the heme methyls of the protohemin IX at the active site of this protein is shown in Figure 8. Although it is likely that our estimation of the axial dipolar contribution to the isotropic shifts is not quantitatively correct, we find that *if it behaves the simple Curie law*, only the values of the spin densities, and not the value of ΔE_π , are affected by the size of the axial dipolar term. However, the assumption that the dipolar shift behaves the simple Curie law when the contact shift does not may not be realistic. Indeed, as mentioned above, the two-level situation, where the orbitals differ in orientation by 90° , requires opposite signs for the in-plane (rhombic) magnetic anisotropy for ground and excited states and hence an apparent twisting of the orientation of the major in-plane magnetic axis and diminution in the anisotropy as the excited state becomes thermally populated. It is, however, difficult to imagine how this behavior of the rhombic dipolar shift could cause the axial dipolar shift to exhibit non-Curie behavior. Interpretation of the dipolar shifts of the protons of protein side chains may allow quantitative analysis of the temperature dependence of the axial and rhombic dipolar shifts of heme resonances and an unambiguous calculation of true contact shifts and spin densities in the *Aplysia* metMbCN system.⁴⁶ For the present, the fit to the experimental data shown in Figure 8 represents a simple interpretation of the temperature

dependence of the methyl proton signals of *Aplysia* metMbCN, to which later more sophisticated treatments may be compared.

The temperature dependence of most of the hyperfine-shifted resonances of rabbit ferricytochrome *b*₅ was measured at 220 MHz by continuous wave techniques in 1972 by Keller and Wüthrich.²² By extracting the data from the published Curie plot (Figure 4 of ref 22a) and fitting the three resolved heme methyl resonances to eq 8, acceptable fits are obtained for energies ranging from 400 to 700 cm⁻¹. The small temperature range of the measurements (7–37 °C) and the inherent errors in both the original measurements and in our ability to estimate the chemical shifts from the Curie plot prevent a more exact value of ΔE_π from being determined, but it is at least clear that the value is large compared to $k_B T$ at room temperature, and of a similar magnitude to the energy separation, V , between the d_{xz} and d_{yz} orbitals, calculated from EPR g values ($V = 540$ – 800 cm⁻¹) using the three-level approach first developed by Griffith,⁴⁷ where the three d-orbitals formerly of t_{2g} symmetry are mixed by spin-orbit coupling and the ligand field. The similarity in energy separations calculated from EPR g values measured at 4 K and estimated from NMR spectra measured at ambient temperatures is highly satisfying.

Summary. In this work we have adapted the Curie law to the case of systems with one or more thermally accessible excited states and have developed and tested a fitting program that uses the isotropic shifts of all available resonance lines for a paramagnetic complex to determine the best estimate of the energy separation, ΔE_π for the most common situation, that of only one thermally accessible excited state, as well as the best estimates of the spin density coefficients for the ground and excited states. We have applied this treatment to experimental data reported previously for several model hemins and two heme proteins and have found that the values of ΔE_π obtained are quantitatively reasonable in terms of our expectations, based upon the energy separations calculated from EPR g values for the systems of interest. For cyanometmyoglobin the g values predict an energy separation of the d_π orbitals, V , of 0.92λ ,⁴⁵ where λ is the spin-orbit coupling constant for low-spin d^5 . The free-ion value of λ for low-spin Fe(III) is 460 cm⁻¹,⁴⁸ and others have reduced this value to 340³² or 300 cm⁻¹⁴⁹ to account for covalency effects. We previously used 400 cm⁻¹ (87% of the free-ion value).⁸ Using 300–400 cm⁻¹ as reasonable boundaries for the value of λ predicts $V = \Delta E_\pi = 275$ – 370 cm⁻¹, while the best fit obtained from the NMR data for *Aplysia* cyanometmyoglobin¹⁵ is 450–550 cm⁻¹, a satisfactory comparison, at least at the high end. For bis(histidine) or *N*-MeIm coordinated hemes, whether in ferricytochrome *b*₅ or the model hemins studied previously in this laboratory,^{1–12} the separation in energy of the two d_π orbitals, V , calculated from EPR g values, is 1.8– 2.0λ ,⁵⁰ or 540–800 cm⁻¹, while the range of possible values obtained by fitting the three resolved methyl resonances of ferricytochrome *b*₅ is 400–700 cm⁻¹; the values of ΔE_π obtained for model hemins with one fixed axial ligand are 214 and 310 cm⁻¹ for the systems shown in Figures 5 and 6, respectively, and those for model hemins having freely rotating axial ligands are 77 cm⁻¹ for the system shown in Figure 4 and too small to measure for many other systems, including those shown in Figure 3. Thus, even though the energy separation, V , calculated from EPR g values is much larger (540–800 cm⁻¹), the apparent value of ΔE_π is much smaller in each of these model heme cases because of rapid interchange of proton unpaired electron spin densities due to rapid rotation (or libration in the case of the systems shown in Figures 5 and 6) of the axial ligands. This rapid interchange is clearly fast on the NMR time scale, and its effect is to partially

average the extreme differences in spin densities for symmetry-related protons. Fitting the observed isotropic shift data leads to a smaller apparent ΔE_π in these systems. Since rotation of the axial histidine(s) provided by the heme proteins is not possible, the fits of their isotropic shift data yield the expected ΔE_π for the ligand set. Therefore, it is not necessary to postulate the rapid interconversion of several structures¹⁵ of *Aplysia* cyanometmyoglobin or any other heme protein in order to account for the observed “non-Curie” temperature dependence of the heme resonances. Furthermore, we may anticipate that the rhombic dipolar contribution to the isotropic shifts of low-spin ferriheme systems will also show “non-Curie”, and even “anti-Curie”, behavior because the sign of the rhombic dipolar shift for any given heme substituent will be opposite in sign for the excited state as compared to the ground state. In contrast, the axial dipolar shift should obey the simple Curie law, at least if χ_{zz} is normal to the plane of the heme. This same theoretical treatment and fitting procedure could be applied to the NMR spectra of any other system having one or more thermally accessible excited states, including complexes having spin-admixed $S = 3/2$ and $5/2$ ground states, as we will show elsewhere.⁵¹ In fact, the temperature dependences of the isotropic shifts of the protons of antiferromagnetically coupled complexes should also follow the predictions of eq 8, since the Bleaney–Bowers expression⁵² is a special case of that equation in which $F_{n,1} = 0$ if the ground state is $S = 0$, and the weighting factors W_1 and W_2 of eq 8 are determined by the spin states of the ground and excited states, in accord with the tabulated values for the Bleaney–Bowers expression.⁵²

Acknowledgment. The support of the National Institutes of Health, Grant DK 31038 (F.A.W.), is gratefully acknowledged.

References and Notes

- (1) Walker, F. A. *J. Am. Chem. Soc.* **1980**, *102*, 3254–3256.
- (2) Walker, F. A.; Balke, V. L.; McDermott, G. A. *J. Am. Chem. Soc.* **1982**, *104*, 1569–1574.
- (3) Walker, F. A.; Benson, M. *J. Phys. Chem.* **1982**, *86*, 3495–3499.
- (4) Lin, Q.; Simonis, U.; Tipton, A. R.; Norvell, C. J.; Walker, F. A. *Inorg. Chem.* **1992**, *31*, 4216–4217.
- (5) Tan, H.; Simonis, U.; Shokhirev, N. V.; Walker, F. A. *J. Am. Chem. Soc.* **1994**, *116*, 5784–5790.
- (6) Isaac, M. F.; Lin, Q.; Simonis, U.; Suffian, D. J.; Wilson, D. L.; Walker, F. A. *Inorg. Chem.* **1993**, *32*, 4030–4041.
- (7) Walker, F. A.; Simonis, U. Proton NMR Spectroscopy of Model Hemes. In *Biological Magnetic Resonance*; Berliner, L. J., Reuben, J., Eds.; Plenum Press: New York, 1993; Vol. 12, pp 133–274.
- (8) Walker, F. A.; Huynh, B. H.; Scheidt, W. R.; Osvath, S. R. *J. Am. Chem. Soc.* **1986**, *108*, 5288–5297.
- (9) Zhang, H.; Simonis, U.; Walker, F. A. *J. Am. Chem. Soc.* **1990**, *112*, 6124–6126.
- (10) Simonis, U.; Dallas, J. L.; Walker, F. A. *Inorg. Chem.* **1992**, *31*, 5349–5350.
- (11) Walker, F. A.; Simonis, U.; Zhang, H.; Walker, J. M.; Ruscitti, T. M.; Kipp, C.; Amputch, M. A.; Castillo, B. V.; Cody, S. H.; Wilson, D. L.; Graul, R. E.; Yong, G. J.; Tobin, K.; West, J. T.; Barichievich, B. A. *New J. Chem.* **1992**, *16*, 609–620.
- (12) Basu, P.; Shokhirev, N. V.; Enemark, J. H.; Walker, F. A. *J. Am. Chem. Soc.* **1995**, *117*, 9042–9055.
- (13) La Mar, G. N. In *Biological Application of Magnetic Resonance*; Shulman, R. B., Ed.; Academic Press: New York, 1979; p 305.
- (14) McLachlan, S. J.; La Mar, G. N.; Lee, K.-B. *Biochim. Biophys. Acta* **1988**, *957*, 430.
- (15) Peyton, D. H.; La Mar, G. N.; Pande, U.; Ascoli, F.; Smith, K. M.; Pandey, R. K.; Parish, D. W.; Bolognesi, M.; Brunori, M. *Biochemistry* **1989**, *28*, 4880–4887.
- (16) (a) Satterlee, J. D. *Annu. Rep. NMR Spectrosc.* **1986**, *17*, 79. (b) Satterlee, J. D. In *Metal Ions in Biological Systems*; Sigel, H., Ed.; Marcel Dekker: New York, 1986; Vol. 21, p 121.
- (17) Satterlee, J. D.; Alam, S.; Yi, Q.; Erman, J. E.; Constantinidis, I.; Russel, D. J.; Moench, S. J. Proton NMR studies of Selected Paramagnetic Heme Proteins. In *Biological Magnetic Resonance*; Berliner, L. J., Reuben, J., Eds.; Plenum Press: New York, 1993; Vol 12, pp 275–298.

- (18) (a) Turner, D. L. *Eur. J. Biochem.* **1993**, *211*, 563. (b) Santos, H.; Turner, D. L. *Magn. Reson. Chem.* **1993**, *31*, S90.
- (19) Santos, H.; Turner, D. L. *Biochim. Biophys. Acta* **1988**, *954*, 277–286.
- (20) Bertini, I.; Luchinat, C. In *NMR of Paramagnetic Molecules in Biological Systems*; Bowen, D. L., Hubit, G., Myson-Etherington, D., Eds.; Benjamin-Cummings: Menlo Park, CA, 1986.
- (21) (a) Keller, R. M.; Wüthrich, K. *Biochim. Biophys. Acta* **1978**, *533*, 195–208. (b) Keller, R. M.; Schejter, A.; Wüthrich, K. *Ibid.* **1980**, *626*, 15–22. (c) Moore, G. R.; Williams, R. J. P. *Eur. J. Biochem.* **1980**, *103*, 523–532. (d) Keller, R. M.; Wüthrich, K. *Biochim. Biophys. Acta* **1981**, *668*, 307–320. (e) Senn, H.; Eugster, A.; Wüthrich, K. *Ibid.* **1983**, *743*, 58–68. Senn, H.; Wüthrich, K. *Ibid.* **1983**, *743*, 69–81. (f) Senn, H.; Wüthrich *Ibid.* **1983**, *746*, 48–60. (g) Senn, H.; Cusanovich, M. A.; Wüthrich, K. *Ibid.* **1984**, *785*, 46–53. (h) Moore, G. R.; Williams, G. *Ibid.* **1984**, *788*, 147–150. (i) Senn, H.; Böhme, H.; Wüthrich, K. *Ibid.* **1984**, *789*, 311–323. (j) Moench, S. J.; Satterlee, J. D. *J. Biol. Chem.* **1989**, *264*, 9923–9931. (k) Wand, A. J.; Di Stefano, D. L.; Feng, Y.; Roder, H.; Englander, S. W. *Biochemistry* **1989**, *28*, 186–194. (l) Feng, Y.; Roder, H.; Englander, S. W.; Wand, A. J.; Di Stefano, D. L. *Ibid.* **1989**, *28*, 195–203. (m) Feng, Y.; Roder, H.; Englander, S. W. *Biophys. J.* **1990**, *57*, 15–22. (n) Ferrer, J. C.; Guillemette, J. G.; Bogumil, R.; Inglis, S. C.; Smith, M.; Mauk, A. G. *J. Am. Chem. Soc.* **1993**, *115*, 7507–7508. (o) Timkovich, R.; Cai, M. *Biochemistry* **1993**, *32*, 11516–11523. (p) Yi, Q.; Satterlee, J. D.; Erman, J. E. *Magn. Reson. Chem.* **1993**, *31*, S53–S58.
- (22) (a) Keller, R. M.; Wüthrich, K. *Biochim. Biophys. Acta* **1972**, *285*, 326–336. (b) Keller, R. M.; Wüthrich, K. *Ibid.* **1980**, *621*, 204–217. (c) La Mar, G. N.; Burns, P. D.; Jackson, J. T.; Smith, K. M.; Langry, K. C.; Strittmatter, P. *J. Biol. Chem.* **1981**, *256*, 6075–6079. (d) McLachlan, S. J.; La Mar, G. N.; Lee, K.-B. *Biochim. Biophys. Acta* **1988**, *957*, 430–445. (e) Pochapsky, T. C.; Sligar, S. G.; McLachlan, S. J.; La Mar, G. N. *J. Am. Chem. Soc.* **1990**, *112*, 5258–5263. (f) Veitch, N. C.; Whitford, D.; Williams, R. J. P. *FEBS Lett.* **1990**, *269*, 297–304. (g) Lee, K.-B.; La Mar, G. N.; Kehres, L. A.; Fujinari, E. M.; Smith, K. M.; Pochapsky, T. C.; Sligar, S. G. *Biochemistry* **1990**, *29*, 9623–9631. (h) Lee, K.-B.; Jun, E.; La Mar, G. N.; Rezzano, I. N.; Pandey, R. K.; Smith, K. M.; Walker, F. A.; Buttlare, D. H. *J. Am. Chem. Soc.* **1991**, *113*, 3576–3583. (i) Rivera, M.; Barillas-Mury, C.; Christensen, K. A.; Little, J. W.; Wells, M. A.; Walker, F. A. *Biochemistry* **1993**, *32*, 622–627.
- (23) (a) Moura, J. J. G.; Santos, H.; Moura, I.; LeGall, J.; Moore, G. R.; Williams, R. J. P.; Xavier, A. V. *Eur. J. Biochem.* **1982**, *127*, 151–155. (b) Guerlesquin, F.; Bruschi, M.; Wüthrich, K. *Biochim. Biophys. Acta* **1985**, *830*, 296–303. (c) Fan, K.; Akutsu, H.; Kyogoku, Y.; Niki, K. *Biochemistry* **1990**, *29*, 2257–2263. (d) Palma, P. N.; Moura, I.; LeGall, J.; Van Beeumen, J.; Wampler, J. E.; Moura, J. J. G. *Ibid.* **1994**, *33*, 6394–6407.
- (24) Gadsby, P. M. A.; Hartshorn, R. T.; Moura, J. J. G.; Sinclair-Day, J. D.; Sykes, A. G.; Thomson, A. J. *Biochim. Biophys. Acta* **1989**, *994*, 37–46.
- (25) Wu, J.-Z.; La Mar, G. N.; Yu, L. P.; Lee, K.-B.; Walker, F. A.; Chiu, M.; Sliger, S. G. *Biochemistry* **1991**, *30*, 2156–2165.
- (26) Saraiva, L. M.; Liu, M. Y.; Payne, W. J.; LeGall, J.; Moura, J. J. G.; Moura, I. *Eur. J. Biochem.* **1990**, *189*, 333–341.
- (27) La Mar, G. N.; de Ropp, J. S. NMR Methodology for Paramagnetic Proteins. In *Biological Magnetic Resonance*; Berlinger, L. J., Reuben, J., Eds.; Plenum Press: New York, 1993; Vol. 12, pp 1–111.
- (28) Longuet-Higgins, H. C.; Rector, C. W.; Platt, R. R. *J. Chem. Phys.* **1950**, *18*, 1174–1181.
- (29) (a) Streitwieser, A., Jr. *Molecular Orbital Theory for Organic Chemists*; John Wiley: New York, 1961. (b) Greenwood, H. H. *Computing Methods in Quantum Organic Chemistry*; Wiley-Interscience: New York, 1972.
- (30) Korsun, Z. R.; Moffat, F.; Frank, K.; Cusanovich, M. A. *Biochemistry* **1982**, *21*, 2253–2258.
- (31) Jesson, J. P. The Paramagnetic Shift. In *NMR of Paramagnetic Molecules*; La Mar, G. N., Horrocks, W. D., Holm, R. H., Eds.; Academic Press: New York, 1973; p 2.
- (32) Horrocks, W. D.; Greenberg, E. S. *Biochim. Biophys. Acta* **1973**, *322*, 38–44; *Mol. Phys.* **1974**, *27*, 993–999.
- (33) La Mar, G. N.; Walker, F. A. In *The Porphyrins*; Dolphin, D., Ed.; Academic Press: New York, 1979; pp 61–157 and references therein.
- (34) Moss, T. H.; Bearden, A. J.; Bartsch, R. G.; Cusanovich, M. A. *Biochemistry* **1968**, *7*, 1583–1591.
- (35) Maltempo, M. M. *J. Chem. Phys.* **1974**, *61*, 2540–2547.
- (36) Maltempo, M. M.; Moss, T. H. *Q. Rev. Biophys.* **1976**, *9*, 181–215.
- (37) Goff, H. M.; Shimomura, E. *J. Am. Chem. Soc.* **1980**, *102*, 31–37.
- (38) Boersma, A. D.; Goff, H. M. *Inorg. Chem.* **1982**, *21*, 581–586.
- (39) (a) Toney, G. E.; ter Haar, L. W.; Savrin, J. E.; Gold, A.; Hatfield, W. E.; Sangiah, R. *Inorg. Chem.* **1984**, *23*, 2561–2563. (b) Toney, G. E.; Gold, A.; Savrin, J.; ter Haar, L. W.; Sangiah, R.; Hatfield, W. E. *Ibid.* **1984**, *23*, 4350–4352.
- (40) McConnell, H. M. *J. Chem. Phys.* **1956**, *24*, 764.
- (41) Press, W. H.; Teukolsky, S. A.; Vetterling, W. T.; Flannery, B. P. *Numerical Recipes*; Cambridge University Press: Cambridge, UK, 1986; p 342.
- (42) Forsythe, G. E.; Malcolm, M. A.; Moler, C. B. *Computer Methods for Mathematical Computations*; Prentice-Hall: Englewood Cliffs, NJ, 1977.
- (43) La Mar, G. N.; Walker, F. A. *J. Am. Chem. Soc.* **1972**, *94*, 8607–8608.
- (44) Walker, F. A.; Lo, M.-W.; Ree, M. T. *J. Am. Chem. Soc.* **1976**, *98*, 3484–3489.
- (45) Hori, H. *Biochim. Biophys. Acta* **1971**, *251*, 227.
- (46) La Mar, G. N. Personal communication.
- (47) Griffith, J. S. *Nature* **1957**, *180*, 30; *Mol. Phys.* **1971**, *21*, 135.
- (48) Figgis, B. N.; Lewis, J. In *Techniques of Inorganic Chemistry*; Jonassen, H. B., Weissberger, A., Eds.; Wiley Interscience: New York, 1965; Vol. IV, p 159.
- (49) Maltempo, M. M. *J. Chem. Phys.* **1974**, *61*, 2540–2547.
- (50) Walker, F. A.; Reis, D.; Balke, V. L. *J. Am. Chem. Soc.* **1984**, *106*, 6888–6898.
- (51) Nasset, M. J. M.; Shokhirev, N. V.; Shokhireva, T. Kh.; Watson, C. T.; Walker, F. A. Manuscript in preparation.
- (52) O'Connor, C. J. Magnetochemistry—Advances in Theory and Experimentation. In *Progress in Inorganic Chemistry*; Lippard, S. J., Ed.; Wiley-Interscience: New York, 1982; Vol. 29, pp 203–283.